

# Supporting Information for ”Decadal variability of eddy temperature fluxes in the Labrador Sea”

Christopher Danek<sup>1,2</sup> \*, Patrick Scholz<sup>1</sup> and Gerrit Lohmann<sup>1,2</sup>

<sup>1</sup>Alfred Wegener Institute for Polar and Marine Research (AWI), Bremerhaven, Germany

<sup>2</sup>MARUM-Center for Marine Environmental Sciences, Bremen, Germany

## Contents of this file

1. Text S1
2. Figures S1 to S3

---

\* Alfred Wegener Institute for Polar and  
Marine Research, Am Handelshafen 12,  
27570 Bremerhaven, Germany

**Text S1.** The global Finite Element Sea ice–Ocean Model FESOM (Wang et al., 2014) solves the governing equations for the ocean and sea ice on the vertices of tetrahedral elements of irregular size, i.e. an Arakawa-A-like grid. A subgrid-scale (SGS) flux for parameterizing the eddy effects tracer mixing along isopycnals (Redi, 1982) and advection due to adiabatic stirring (Gent & McWilliams, 1990) is enabled in both model configurations and scaled with the local horizontal resolution and stratification of the flow. Diapycnal mixing is implemented via the  $k$ -profile parameterization (KPP; Large et al., 1994). For salinity, a flux correction was applied at the sea surface towards climatological values with a (moderate) velocity of  $50 \text{ m } 300 \text{ days}^{-1}$ . Further model specifications can be found in Danek, Scholz, and Lohmann (2019) and Wang et al. (2014). At the sea surface, FESOM was driven by the  $\sim 1.8^\circ \times \sim 1.8^\circ$  atmospheric reanalysis dataset CORE-II in an 6-hourly interval (the regular forcing data was bilinear interpolated to the irregular FESOM grids; Large & Yeager, 2009). According to the CORE (Griffies et al., 2012) and OMIP (Griffies et al., 2016) protocols, we integrated FESOM for five full 62-year long cycles from 1948-2009. The first cycle was initialized from the PHC3 dataset (Steele et al., 2001) and the subsequent cycles were initialized from the last time step of the previous cycle. All shown analysis are based on the fifth, i.e. last, cycle.

To analyze the resolution-dependence of the involved dynamical processes during MLD restratification, low- and high-resolution FESOM grids were designed (Fig. S1). Based on a global average horizontal resolution of 130 (40) km, the element size was reduced to 40 (20) km along the coasts and the equator in the low (high) -resolution setup to improve the modeling of upwelling. Upon this, the resolution was further reduced in the subpolar gyre, the Arctic Ocean, deep convection areas and along the Greenland coast.

The low-resolution grid with 39 vertical levels was utilized in earlier FESOM experiments and showed good agreement with the LS deep water variability compared to observations, albeit missing fluxes between the boundary current and the LS interior (Scholz et al., 2014). In the high-resolution setup with 61 vertical levels, the element size was reduced in the North Atlantic where measured 1) SSH variability is high (AVISO), 2) bottom slopes are steep (Amante & Eakins, 2009) and 3) horizontal temperature gradients in 200 m depth are large (Locarnini et al., 2013). With these constraints we ensured an appropriate representation of important dynamic processes related to mesoscale eddies, fronts, boundary currents, upwelling, and topographic features.

## References

- Amante, C., & Eakins, B. W. (2009). *ETOPO1 1 Arc-Minute Global Relief Model: Procedures, Data Sources and Analysis* (NOAA Technical Memorandum NESDIS No. NGDC-24). NOAA. ([July 15 2015]) doi: 10.7289/V5C8276M
- Danek, C., Scholz, P., & Lohmann, G. (2019). Effects of High Resolution and Spinup Time on Modeled North Atlantic Circulation. *Journal of Physical Oceanography*, 49(5), 1159-1181. doi: 10.1175/JPO-D-18-0141.1
- Gent, P. R., & McWilliams, J. C. (1990). Isopycnal Mixing in Ocean Circulation Models. *Journal of Physical Oceanography*, 20(1), 150-155. doi: 10.1175/1520-0485(1990)020<0150:IMIOCM>2.0.CO;2
- Griffies, S. M., Danabasoglu, G., Durack, P. J., Adcroft, A. J., Balaji, V., Böning, C. W., ... Yeager, S. G. (2016). OMIP contribution to CMIP6: experimental and diagnostic protocol for the physical component of the Ocean Model Intercomparison Project. *Geoscientific Model Development*, 9(9), 3231-3296. doi: 10.5194/gmd-9-3231-2016

- Griffies, S. M., Winton, M., Samuels, B., Danabasoglu, G., Yeager, S. G., Marsland, S. J., ... Bentsen, M. (2012). *Datasets and protocol for the CLIVAR WGOMD Coordinated Ocean-sea ice Reference Experiments (COREs)* (WCRP Report No. No. 21/2012).
- Kelley, D., & Richards, C. (2021). oce: Analysis of Oceanographic Data [Computer software manual]. Retrieved from <https://CRAN.R-project.org/package=oce> (R package version 1.4-0)
- Large, W. G., McWilliams, J. C., & Doney, S. C. (1994). Oceanic vertical mixing: A review and a model with a nonlocal boundary layer parameterization. *Review of Geophysics*, *32*(4), 363-403. doi: 10.1029/94RG01872
- Large, W. G., & Yeager, S. G. (2009). The global climatology of an interannually varying air-sea flux data set. *Journal of Climate*, *33*(341). doi: 10.1007/s00382-008-0441-3
- Locarnini, R. A., Mishonov, A. V., Antonov, J. I., Boyer, T. P., Garcia, H. E., Baranova, O. K., ... Seidov, D. (2013). *World Ocean Atlas 2013, Volume 1: Temperature*. S. Levitus. Ed., A. Mishonov technical editor, NOAA Atlas NESDIS 73.
- Redi, M. H. (1982). Oceanic Isopycnal Mixing by Coordinate Rotation. *Journal of Physical Oceanography*, *12*(10), 1154-1158. doi: 10.1175/1520-0485(1982)012<1154:OIMBCR>2.0.CO;2
- Scholz, P., Kieke, D., Lohmann, G., Ionita, M., & Rhein, M. (2014). Evaluation of Labrador Sea Water formation in a global Finite-Element Sea-Ice Ocean Model setup, based on a comparison with observational data. *Journal of Geophysical Research: Oceans*, *119*(3), 1644-1667. doi: 10.1002/2013JC009232
- Steele, M., Morley, R., & Ermold, W. (2001). PHC: A Global Ocean Hydrography with a High-Quality Arctic Ocean. *Journal of Climate*, *14*(9), 2079-2087. doi: 10.1175/

1520-0442(2001)014<2079:PAGOHW>2.0.CO;2

Wang, Q., Danilov, S., Sidorenko, D., Timmermann, R., Wekerle, C., Wang, X., ...

Schröter, J. (2014). The Finite Element Sea Ice-Ocean Model (FESOM) v.1.4: formulation of an ocean general circulation model. *Geoscientific Model Development*, 7(2), 663-693. doi: 10.5194/gmd-7-663-2014

Wekerle, C., Wang, Q., von Appen, W.-J., Danilov, S., Schourup-Kristensen, V., & Jung,

T. (2017). Eddy-Resolving Simulation of the Atlantic Water Circulation in the Fram Strait With Focus on the Seasonal Cycle. *Journal of Geophysical Research: Oceans*, 122(11), 8385-8405. doi: 10.1002/2017JC012974

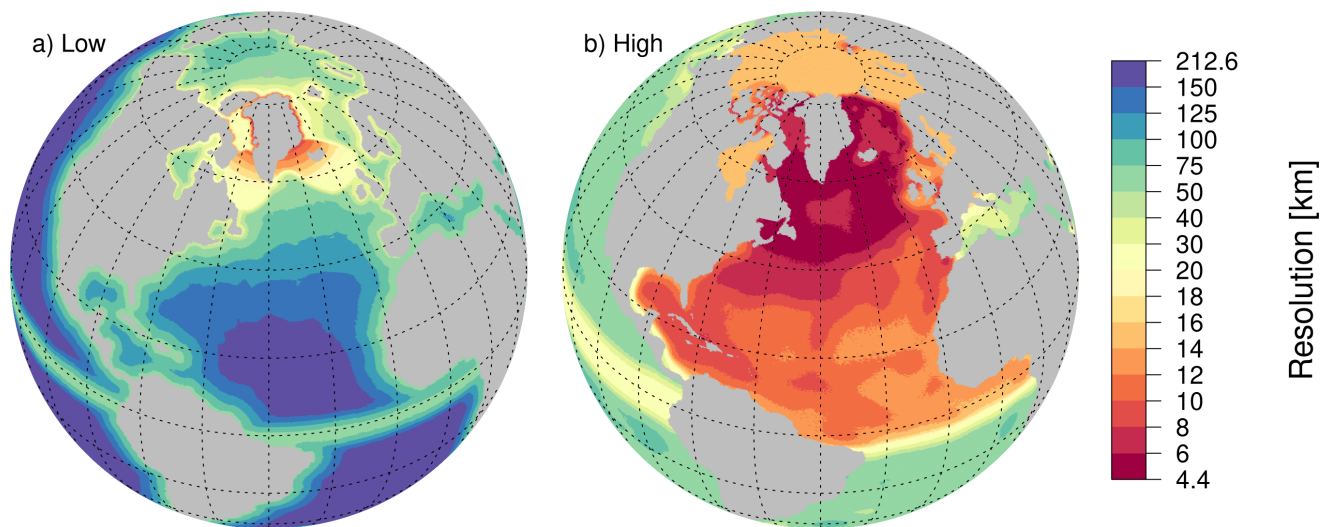


**Figure S1.** Colors show horizontal resolution (in km) of the utilized low- (left) and high-resolution (right) FESOM setups. See Text S1 for details. Orthographic projection realized with the R package "oce" (Kelley & Richards, 2021).

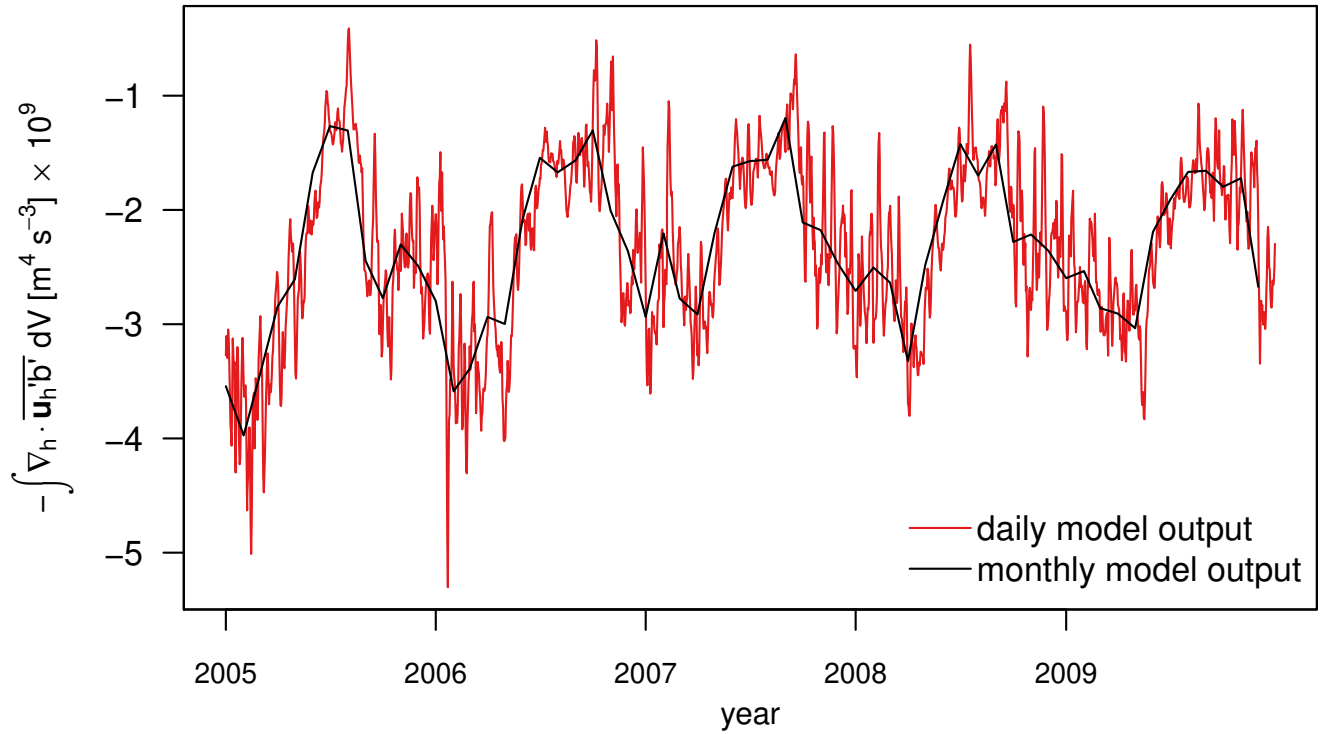


**Figure S2.** Eddy component of horizontal buoyancy advection divergence volume-integrated over a box located at Fram Strait ( $-20$  to  $20^{\circ}\text{E}$ ,  $76$  to  $82^{\circ}\text{N}$ ) calculated based on monthly (black) or daily (red) model output (larger values indicate buoyancy gain in summer; see methods section for eddy component calculation). Model data taken from another FESOM run with the same model version and parameters as in this study (Wekerle et al., 2017).

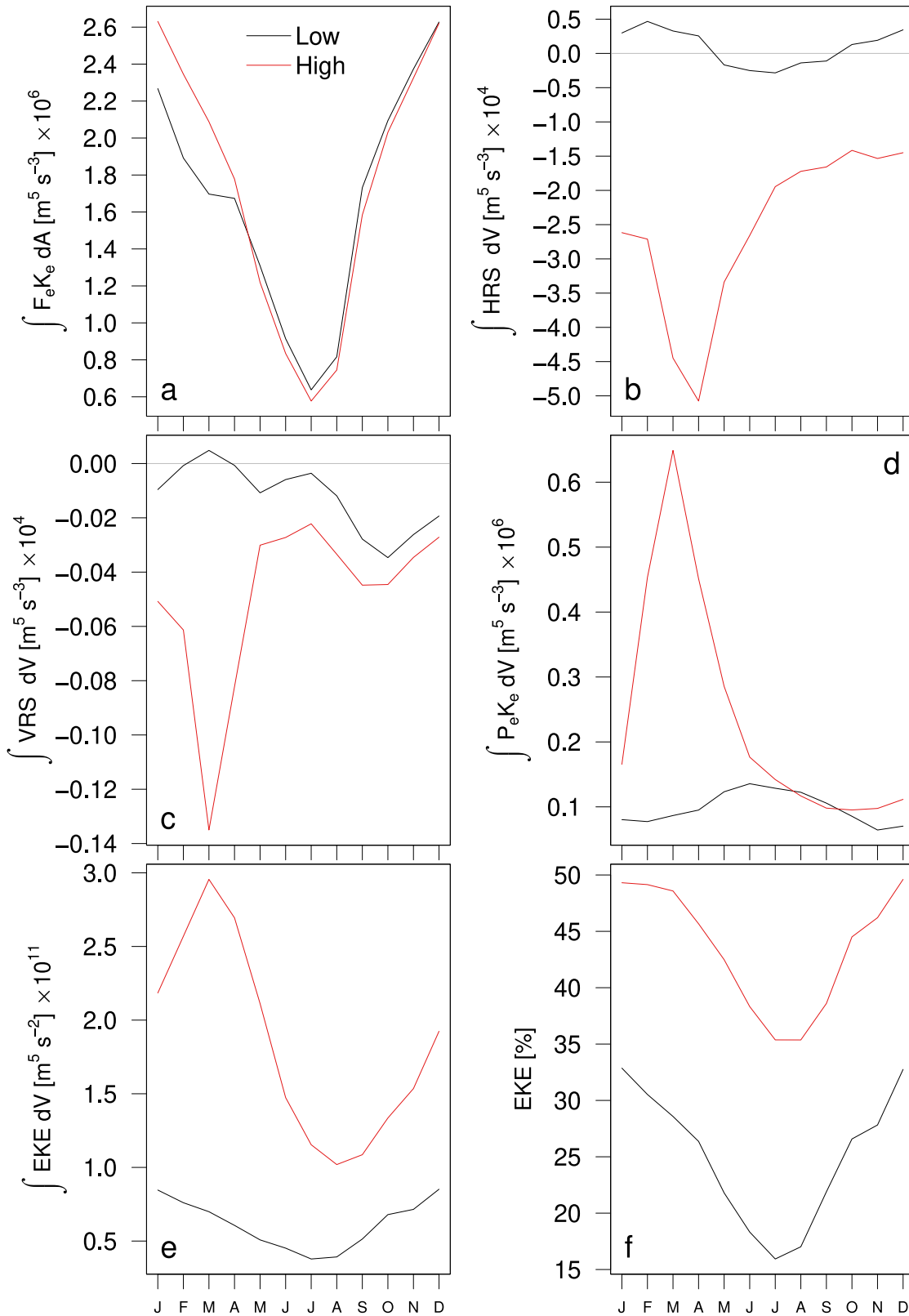


**Figure S3.** Average (1948-2009) seasonal cycle of low- (black) and high-resolution (red) EKE changes due to a) area-integrated eddy wind work at the sea surface  $F_e K_e$ , b) horizontal (HRS), c) vertical barotropic (VRS) and d) baroclinic  $P_e K_e$  volume-integrated instabilities in the LS interior (index area shown in Fig. 1 a,b; positive values indicate an EKE generation; different y-axes). e,f) show the volume-integrated EKE and its contribution to total kinetic energy.

May 28, 2021, 11:45am